

FOURIER-GALERKIN METHOD FOR LOCALIZED SOLUTIONS OF THE SIXTH-ORDER GENERALIZED BOUSSINESQ EQUATION

M. A. CHRISTOU AND C. I. CHRISTOV

ABSTRACT. A complete orthonormal system of functions in $L^2(-\infty, \infty)$ is used as a basis function in a Fourier-Galerkin spectral technique for computing localized solutions. The Sixth-Order Generalized Boussinesq Equation is featured whose solutions comprise monotone shapes (*sech*-es) and damped oscillatory shapes (Kawahara solitons). Localized solutions are obtained here numerically and shown to agree quantitatively very well to the known analytical and/or numerical ones. The rate of convergence and truncation error are thoroughly examined.

1. Introduction. In the recent years a number of physical problems have frequently led to boundary value problems in infinite domains. These are the cases when no boundary conditions are specified at certain points, but rather the solution is required to possess a summable square over the infinite domain. Then the solution is said to belong to the $L^2(-\infty, \infty)$ space. A typical example is furnished by the soliton solutions of different nonlinear evolution equations or generalized wave equations. Difference and FEM numerical methods are faced with formidable difficulties when applied to problems in $L^2(-\infty, \infty)$. It suffices to mention the inevitable reducing of the infinite interval to a finite one which introduces artificial eigenvalue problems the latter being irrelevant to the original infinite domain. It can happen that each of the finite-domain approximations has only a trivial solution, while the original problem possesses a nontrivial one or *vice versa*. Sometimes, the finite-domain problem has a solution only for some denumerable set of intervals of its characteristic length.

One of the ways to surmount these difficulties is to use a spectral method with basis system of localized functions which automatically acknowledge the $L^2(-\infty, \infty)$ condition.

From the known spectral techniques we choose the Galerkin method (for the collocation and/or tau-method see, e.g., [6, 3]). The Galerkin method has the advantage of simplicity of the implementation in comparison with the spectral collocation method or tau-method. This turns out to be crucial for the construction of fast and efficient numerical algorithms. The only problem is that a Galerkin techniques require explicit formulas expressing the products of members of the CON system into series with respect to the system. For instance, the Hermite functions and Laguerre functions do not possess that kind of explicit relation. The first system for which a product formula was derived was proposed in [8]. A Galerkin technique based on the said system was developed in [11] and applied to KdV and KS equations with quadratic nonlinearity. It has been recently applied to 2D problems in [10].

Recently the technique has been extended to equations with cubic nonlinearity [7]. In a sequence of papers Boyd [2, 4] showed a general way of constructing CON systems in $L^2(-\infty, \infty)$ by means of coordinate transformation to finite interval and use of Chebishev polynomials (see [3] for references). In the present paper we further develop the technique with application to higher-order equations and/or for solitary waves with oscillatory shapes.

2. Posing the problem. Consider the Sixth-Order Generalized Boussinesq Equation (6GBE) which was treated in [12]:

$$u_{tt} = \gamma^2 u_{xx} + (u^2)_{xx} + \beta u_{xxxx} + \delta u_{xxxxx}. \quad (1)$$

From physical considerations one shows that the sixth-order dispersion coefficient is always positive $\delta > 0$. Without loss of generality we set $\delta = 1$. The coefficient β of the fourth-order derivative can adopt an arbitrary value (positive, negative, or zero). The case $\beta = 0$ is thoroughly investigated theoretically in [5]. Fourier-Galerkin numerical scheme for $\beta = 0$ is developed in [1]. For this reason we will limit ourselves in the present work to the cases $\beta = \pm 1$.

For the localized solution one has the the following condition which plays the role of a boundary condition,

$$\int_{-\infty}^{\infty} u^2(x; t) dx < \infty. \quad (2)$$

We consider the stationary waves in the moving frame $\xi = x - ct$. Then (2) yields the asymptotic b.c., namely

$$u^{(n)}(t, x) \rightarrow 0, \quad \text{for } \xi \rightarrow \pm\infty, \quad n = 0, 1, \dots \quad (3)$$

After integrating (1) twice, and acknowledging the asymptotic boundary conditions (3) one arrives at the following nonlinear ODE

$$\lambda u + \epsilon u^2 + \beta u_{\xi\xi} + u_{\xi\xi\xi\xi} = 0, \quad \lambda = \gamma^2 - c^2. \quad (4)$$

Models, similar to equation (4) can also be obtained for the moving-frame solution of the Fifth-Order Korteweg-de Vries equation (see [13, 5, 15])

As shown first by Kawahara [13], the dispersion relation for eq.(4) reads

$$\kappa^4 + \beta\kappa^2 + \lambda = 0, \quad \text{i.e.,} \quad \kappa^2 = \frac{1}{2}(-\beta \pm \sqrt{\beta^2 - 4\lambda}). \quad (5)$$

Equation (5) shows that the classification of the stationary solutions should be based on criteria which define the asymptotic behavior of the tails. These criteria depend on the values of λ and β . Before proceeding to the description of the numerical method we mention that scaling the independent variable does not change the nature of the boundary value problem in L^2 . Then upon introducing $\xi = \zeta\eta$ we render the above problem to the following boundary value problem

$$\lambda u + \epsilon u^2 + \frac{\beta}{\zeta^2} u_{\eta\eta} + \frac{\delta}{\zeta^4} u_{\eta\eta\eta\eta} = 0, \quad \int_{-\infty}^{\infty} u^2(\eta) d\eta < +\infty, \quad (6)$$

where the primes stand for differentiation with respect to η . The additional parameter ζ is crucial for the optimization of the method. It's introduction allows one to bring in concert the typical length scales of the employed system of functions and the length-scale of the support of the sought localized solution.

3. **The Complete Orthonormal (CON) system.** The system

$$\rho_n = \frac{1}{\sqrt{\pi}} \frac{(ix-1)^n}{(ix+1)^{n+1}}, \quad n = 0, 1, 2, \dots \quad (7)$$

was introduced by Wiener [14] for the purposes of time-series analysis. The significance of (7) for nonlinear problems was demonstrated in [8], where the product formula was derived

$$\rho_n \rho_k = \frac{\rho_{n+k} - \rho_{n-k}}{2\sqrt{\pi}} \quad (8)$$

and the two real-valued subsequences of odd functions S_n and even functions C_n were introduced, namely

$$S_n = \frac{\rho_n + \rho_{-n-1}}{i\sqrt{2}}, \quad C_n = \frac{\rho_n - \rho_{-n-1}}{\sqrt{2}}. \quad (9)$$

Using (8) one easily shows that the products of members of the real-valued sequences are expanded in series with respect to the system as follows (see, [8]):

$$C_n C_k = \frac{1}{2\sqrt{2\pi}} [C_{n+k+1} - C_{n+k} - C_{n-k} + C_{n-k-1}], \quad (10)$$

$$S_n S_k = \frac{1}{2\sqrt{2\pi}} [C_{n+k+1} - C_{n+k} + C_{n-k} - C_{n-k-1}], \quad (11)$$

$$S_n C_k = \frac{1}{2\sqrt{2\pi}} [-S_{n+k+1} + S_{n+k} + S_{n-k} - S_{n-k-1}]. \quad (12)$$

Generalization of these product formulas to the case of triple products can be found in [7].

For the second and fourth derivatives of the basis functions one has (see [8, 9])

$$\begin{aligned} C_n'' &= \sum_{m=0}^{\infty} \chi_{m,n} C_m, & S_n'' &= \sum_{m=0}^{\infty} \chi_{m,n} S_m, & \text{where} \\ \chi_{m,n} &= -\frac{n(n-1)}{4} \delta_{m,n-2} + n^2 \delta_{m,n-1} - \frac{(n+1)(n+2)}{4} \delta_{m,n+2} \\ &\quad - \frac{n^2 + (2n+1)^2 + (n+1)^2}{4} \delta_{m,n} + (n+1)^2 \delta_{m,n+1}, \end{aligned} \quad (13)$$

$$\begin{aligned} C_n'''' &= \sum_{m=0}^{\infty} \omega_{m,n} C_m, & S_n'''' &= \sum_{m=0}^{\infty} \omega_{m,n} S_m, & \text{where} \\ \omega_{m,n} &= \frac{n(n-1)(n-2)(n-3)}{16} \delta_{m,n-4} - \frac{n(n-1)^2(n-2)}{2} \delta_{m,n-3} \\ &\quad - \frac{n(n-1)(7n^2-7n+4)}{4} \delta_{m,n-2} - \frac{n^2(7n^2+5)}{2} \delta_{m,n-1} \\ &\quad + \frac{35n^4+70n^3+85n^2+50n+12}{8} \delta_{m,n} \\ &\quad - \frac{(n+1)^2[7(n+1)^2+5]}{2} \delta_{m,n+1} - \frac{(n+1)(n+2)^2(n+3)}{2} \delta_{m,n+3} \\ &\quad + \frac{(n+1)(n+2)[7(n+1)^2+7(n+1)+4]}{4} \delta_{m,n+2} \\ &\quad + \frac{(n+1)(n+2)(n+3)(n+4)}{16} \delta_{m,n+4}. \end{aligned} \quad (14)$$

4. Algebraic system for the coefficients. The problem admits even functions as solutions and hence we develop the sought solution u into series with respect to the subsequence of functions C_n only, namely

$$u(\eta) = \sum_{n=0}^{\infty} a_n C_n(\eta). \quad (15)$$

Then

$$u''(\eta) = \sum_{m=0}^{\infty} \sum_{n=0}^{\infty} a_m \chi_{m,n} C_n(\eta), \quad u''''(\eta) = \sum_{m=0}^{\infty} \sum_{n=0}^{\infty} a_m \omega_{m,n} C_n(\eta), \quad (16)$$

$$u^2(\eta) = \sum_{m_1=0}^{\infty} \sum_{m_2=0}^{\infty} \sum_{n=0}^{\infty} a_{m_1} a_{m_2} \beta_{m_1 m_2, n} C_n(\eta), \quad \text{where} \quad (17)$$

$$\beta_{nk,m} = \frac{1}{2\sqrt{2\pi}} \left[-\delta_{m,n+k+1} + \delta_{m,n+k} + \delta_{m,|n-k|} - \text{sgn}(|n-k| - \frac{1}{2}) \delta_{m, [|n-k| - \frac{1}{2}]} \right]$$

Introducing (15), (16), and (17) into (6) and combining the terms with the like orthonogonal functions C_n , we obtain the following infinite nonlinear algebraic system for the unknown coefficients a_n :

$$\sum_{m=0}^{\infty} \left[\frac{\delta}{\zeta^4} \omega_{m,n} + \frac{\beta}{\zeta^2} \chi_{m,n} + \lambda \delta_{m,n} \right] a_m - \alpha \sum_{m_1=0}^{\infty} \sum_{m_2=0}^{\infty} a_{m_1} a_{m_2} \beta_{m_1 m_2, n} = 0 \quad (18)$$

In the numerical calculations, a truncated version of the above system is used where the infinity is replaced by N .

5. Algorithm. In order to avoid the trivial solution we consider the re-scaled vector of unknowns $a_i = \alpha \hat{a}_i$ (where α is unknown parameter) and impose a condition on the first coefficient, say $\hat{a}_0 = -1$, which makes the system for coefficients overposed. In order to avoid this problem the equation for \hat{a}_0 should not be used alongside with the rest of the algebraic equations when solving them for \hat{a}_i . Rather, it becomes an equation for determination of α , namely

$$\alpha = \frac{1}{\vartheta} \left[\lambda \hat{a}_0 - \sum_{m=0}^N \hat{a}_m \left(\frac{\beta}{\zeta^2} \chi_{m,0} + \frac{\delta}{\zeta^4} \omega_{m,0} \right) \right], \quad \vartheta \stackrel{\text{def}}{=} \epsilon \sum_{m_1=0}^N \sum_{m_2=0}^N \hat{a}_{m_1} \hat{a}_{m_2} \beta_{m_1 m_2, 0}.$$

The nonlinear system is solved by means of semi-implicit iterative scheme. When the nonlinear term is evaluated the coefficients are treated as known quantities from the previous iteration, namely \hat{a}_i^n, α^n and then the linear system with pentadiagonal matrix is solved for the “new” iteration designated by $\tilde{a}_i, \tilde{\alpha}$:

$$\sum_{m=1}^N \left[\frac{\delta}{\zeta^4} \omega_{m,n} + \frac{\beta}{\zeta^2} \chi_{m,n} + \Delta_{m,n} \right] \tilde{a}_m - \epsilon \alpha^n \sum_{m_1=0}^N \sum_{m_2=0}^N \hat{a}_{m_1}^n \hat{a}_{m_2}^n \beta_{m_1 m_2, k} = 0, \quad (19)$$

$$\tilde{\alpha} = \frac{1}{\vartheta} \left[\lambda \hat{a}_0^n - \sum_{m=0}^N \hat{a}_m^n \left(\frac{\beta}{\zeta^2} \chi_{m,0} + \frac{\delta}{\zeta^4} \omega_{m,0} \right) \right], \quad \vartheta = \epsilon \sum_{m_1=0}^N \sum_{m_2=0}^N \hat{a}_{m_1}^n \hat{a}_{m_2}^n \beta_{m_1 m_2, 0}. \quad (20)$$

In order to control the rate of convergence and to avoid divergence when the process is started from a very rough initial approximation, a relaxation is applied according to the ubiquitous formulas

$$\hat{a}_i^{n+1} = \omega \tilde{a}_i + (1 - \omega) \hat{a}_i^n, \quad \alpha^{n+1} = \omega \tilde{\alpha} + \alpha^n (1 - \omega), \quad 0 < \omega < 1.$$

6. Numerical Results for the Stationary shapes. As has already been mentioned the presence of higher-order derivatives makes the phenomenology of the model richer. In particular, the localized solutions form two distinct classes with different asymptotic behavior of the shape at infinity. One of the classes consists of the ubiquitous monotone *sech*-like shapes while the second comprise shapes whose behavior at infinity is of a damped oscillation (called Kawahara solitons).

One of the main purposes of the present work is to examine the performance of the proposed Fourier-Galerkin technique for the case of non-monotone shapes. In order to reduce the dimension of the parametric space and to make the investigation more focused we set $\gamma = 1$ and $\beta = -1$.

6.1. Monotone Shapes. As shown in [12] the monotone shapes appear for $\beta < -2\sqrt{\lambda}$ with $\lambda > 0$. For example, if $\beta = -1$, the condition for having monotone tails is $c > \sqrt{1 - \frac{1}{4}\beta^2} \approx 0.8660254$. For this case, an analytical solution is available for one particular value of the phase speed, namely

$$u_{an}(\xi) = \frac{105}{169} \frac{\beta^2}{2a} \operatorname{sech}^4 \left(\frac{\xi}{2} \sqrt{\frac{-\beta}{13}} \right), \quad |c| = \sqrt{\gamma^2 - \frac{36}{169}\beta^2} \approx 0.88712. \quad (21)$$

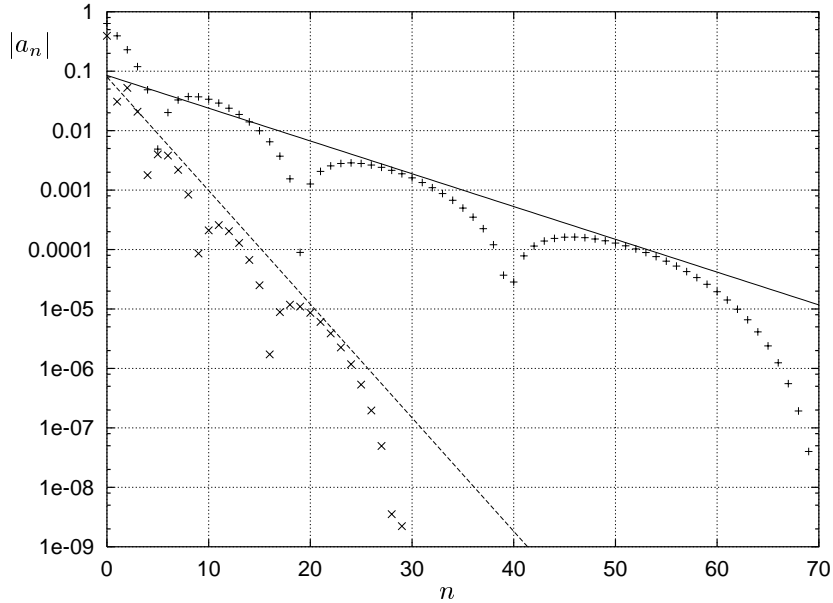


FIGURE 1. Dependence of $|a_n|$ on n for the monotone case as computed with $\zeta = 1$ and $N = 70$. +: $\zeta = 1$, $N = 69$; x: $\zeta = 4$, $N = 29$. Solid line: $a_n = 0.085 \exp[-0.127n]$. Dashed line $a_n = 0.08 \exp[-0.44n]$.

The analytical solution (21) allows us to examine the practical issues of the spectral approximation under consideration, e.g., the speed of convergence and the truncation error. The first problem we attack is calculating the monotone solitary-wave shape for $c = 0.88712$. The result obtained is in very good quantitative agreement with the analytical solution (21). In Figure 1 we show the dependence of

the absolute value of a coefficient on its number n . The decay is clearly exponential with n which is readily verified analytically for a solution of type (21). One sees that the convergence of the series (rate of decay of $|a_n| = e^{-\kappa n}$) is exponential. The best-fit approximation gives for the exponent the value $\kappa = -0.127$.

Now we are able to show the utility of the scale factor ζ . The idea is that for adequately selected ζ the support of the sought localized solution can be brought in concordance with the typical length scale of the employed CON system. Indeed, testing different scales ζ showed that there is a significant impact of the latter on the way the algorithm performs. In the same Figure 1 we present $|a_n(n)|$ also for $\zeta = 4$. The difference is dramatical. The best fit for the exponent of the decay of the coefficients with n is now $\kappa = -0.44$ which means that the exponential convergence is 3.5 faster for $\zeta = 4$ in comparison with $\zeta = 1$.

Apart from the rate of convergence, the next most important characteristics of a spectral method is the truncation error. It allows one to estimate the accuracy with which the solution is obtained as a function of x . When an analytical reference solution is available (which is the case of monotone shapes) then the truncation error is calculated as the difference between the spectral solution and the analytical one at each spatial position x . When an analytical solution is not available one has to calculate the solution with very large number of terms and to use these calculations as a reference (see, Subsection 6.2).

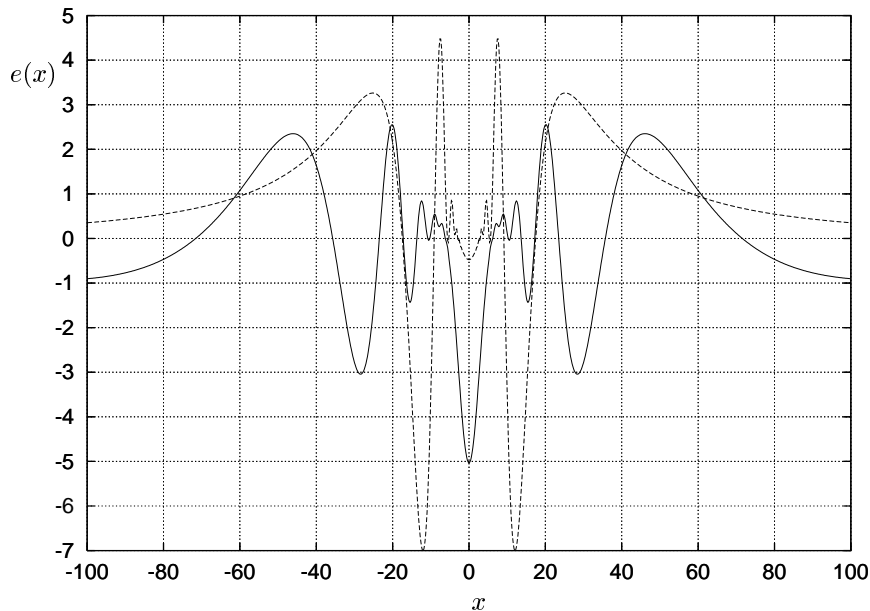


FIGURE 2. Pointwise truncation error for monotone shapes with different scaling factors. Solid line: $10^4 e(x)$ for $\zeta = 4$, $N = 29$. Dashed line: $10^7 e(x)$ for $\zeta = 1$, $N = 69$

In Figure 2 we present the pointwise truncation error for the case $\zeta = 1$ (dashed line) and $\zeta = 4$ (solid line). One sees that in the first case the error is of order of 10^{-4} . This outlines the accuracy of the truncated solution with $N = 39$. For better accuracy one is to use twice as many terms. But then another shortcoming

arises connected with the accumulation of round-off error when the function $u(\eta)$ is evaluated from the series (15), i.e., managing to keep the total number $N+1$ of terms smaller is a valid objective when developing the spectral technique. This means that finding the optimal ζ has not only theoretical significance, but a profound impact on the practical results as well. The pointwise truncation error for $\zeta = 4$ (as presented in the Figure by the solid line) is of *three* orders of magnitudes smaller than the error for $\zeta = 1$. So that, one sees indeed that the proper choice of ζ is of crucial importance for the overall accuracy and the practical efficiency of the method.

6.2. Damped Oscillatory Shapes (Kawahara solitons). For $-2\sqrt{\lambda} \leq \beta \leq 2\sqrt{\lambda}$, damped oscillatory shapes appear. For $\beta > 0$ (say $\beta = 1$) and $\lambda \geq \frac{1}{4}\beta^2$ the wave number k from (5) is a complex number, $k = k_r \pm ik_i$. Then the asymptotic behaviour of the solution at infinity is

$$u = \sin(k_i x + d)e^{-k_r x}.$$

which means that the localized solutions are damped spatial oscillations.

This class of subcritical waves were first discovered by Kawahara numerically in the Fifth-order KdV equation. In Figure 3 the Kawahara solitons are depicted for different values of c . For reasonably small c the damped shapes are well localized (the support of the solution is rather small) and the developed here algorithm is very efficient for their calculation for wide variety of scale factors. The assessment of the truncation error and other issues of the approximation are addressed in a manner similar to the case of monotone shapes.

For $|\beta^2 - 4|\lambda| \ll 1$ (or which is the same, $4|\lambda| = \beta^2 + \varepsilon^2$) the behavior of the solution changes drastically in the sense that it is no longer well localized and now the support L becomes rather large according to the following formula

$$\kappa = \pm \sqrt{\frac{-\beta \pm i\varepsilon}{2}}, \quad \implies \quad k_r \simeq \frac{\varepsilon}{2\sqrt{2}\beta}, \quad \implies \quad L \simeq \varepsilon^{-1} \gg 1.$$

In the case of moderate lengths of the support L , the scaling parameter, ζ , served merely to optimize the method, to make the convergence faster. In the case of long-length support, the solution cannot be obtained without tuning ζ . We demonstrate here the specifics of the technique for this extremely hard case. This way we outline the limits of applicability of the method. The dependence of the solution on the scaling parameter, ζ , is demonstrated in Figure 4.

It is seen that for smaller $\zeta \leq 2$ the full complexity of the tails cannot be resolved and this in its turn affects even the calculated magnitude of the soliton in the center of coordinate system. The number of accurately resolved oscillations in the tails of the solitary wave increases with increasing ζ . $\zeta = 32$ allows a full resolution of the energy containing part of the wave. One sees that increasing ζ twice (from 16 to 32) has a very small quantitative impact on the solution in its energy containing part. Obviously, there is convergence with respect to ζ to the solution of the problem. This result is central to the present work and shows that the selected CON system of functions is a very effective basis function not only in the case of solutions of monotone shapes, but also for solutions with decaying oscillatory tails which are encountered for equations containing higher than the second derivatives.

Turning to the problem of truncation error we mention that for the case of damped oscillatory shapes, an analytical solution does not exist. Hence we calculate the solution using 140 terms ($N = 139$) terms in the series and consider this solution *in lieu* of an analytical one. Then the error function is defined as the difference

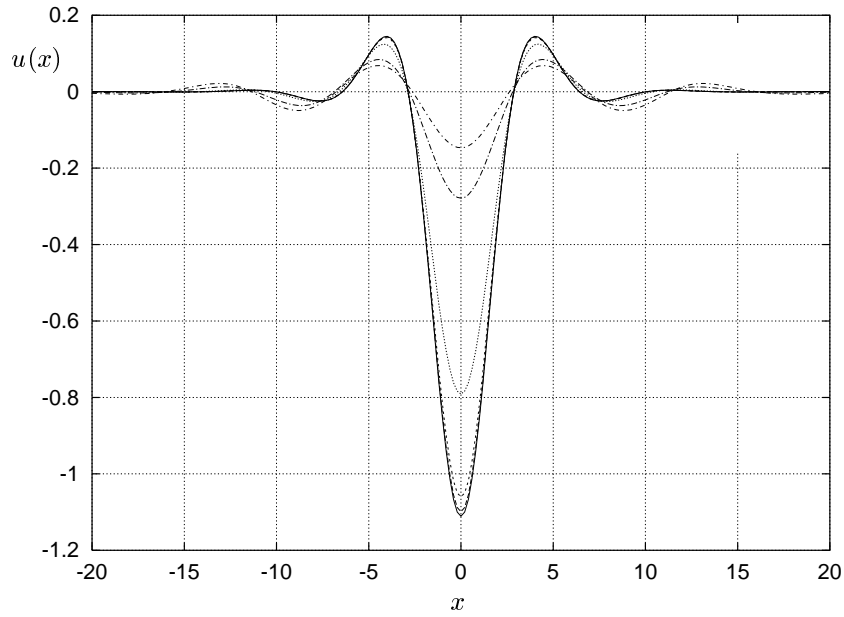


FIGURE 3. Damped oscillatory shapes for different phase speeds:
 ····· $c = 0.85$; - · - · $c = 0.8$; - - - - $c = 0.5$; - - - - $c = 0.2$;
 - - - - $c = 0.1$; ——— $c = 0.01$.

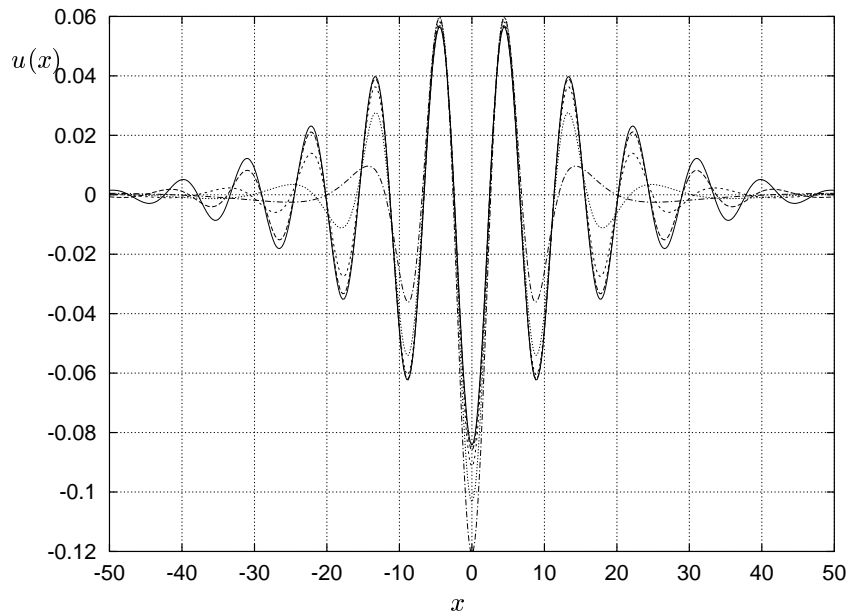


FIGURE 4. Solution for the Kawahara soliton for $c = 0.86$ obtained
 with $N = 39$ and different scaling parameters: - · - · $\zeta = 2$;
 ····· $\zeta = 4$; - - - - $\zeta = 8$; - - - - $\zeta = 16$; ——— $\zeta = 32$.

between the above “more accurate” spectral solution and the spectral solution with the current number of terms.

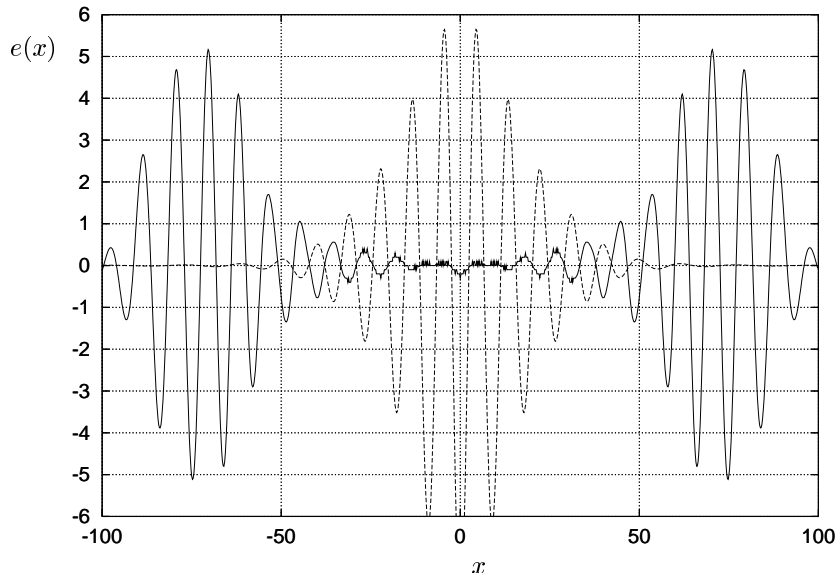


FIGURE 5. Pointwise truncation error for poorly localized Kawahara solitons ($c = 0.86$) as calculated with scale factor $\zeta = 32$. Solid line: $10^4 e(x)$ for $N = 69$. Dashed line: $10^2 e(x)$ for $N = 39$

Once again we focus on the hardest case of poorly localized damped oscillatory shapes for $c = 0.86$. We take for the scaling parameter the above selected value $\zeta = 32$ which takes care of the problem of poor localization. The pointwise truncation error for this case is presented in Figure 5. The error for $N = 39$ is of order of 10^{-2} while for $N = 69$ it is of order of 10^{-4} . This means that provided that the proper scale factor ζ is found, the solution is rather robust with respect to the total number of terms in the truncated series.

Conclusions. In the present paper a Fourier-Galerkin spectral technique is developed for calculating localized solutions of nonlinear equations containing fourth-order derivatives. As a basis is used the complete orthonormal (CON) system previously proposed in the authors works. A scaling parameter is introduced which allows a fine-tuning and optimization of the technique proposed.

A typical physical example where the higher-order derivatives are important is the equation to which are reduced the Sixth-Order Generalized Boussinesq Equation and/or Fifth-Order Korteweg-de Vries equation for stationary propagating localized solution are sought. The localized solutions of this problem are known to form two distinct classes: monotone (*sech*-like) shapes and damped oscillatory shapes (Kawahara solitons).

Iterative algorithm is devised for solving the truncated version of the algebraic system for the coefficients of the Galerkin series. Numerical experiments with different number of terms are conducted for different values of the scaling parameter. These experiments establish the practical convergence of the method and indicate

an exponential decay of the coefficients with the increase of their number (exponential convergence).

The global truncation error is assessed via comparison to an analytical soliton solution for the monotone shapes. Since an analytical solution is not available for the damped oscillatory shapes, a solution with larger number of terms (say 70) is used as a reference. It turns out that the truncation error can be reduced to 10^{-6} in both cases with number of terms as little as 30. For the extreme case of poorly localized damped oscillatory shapes, a number of 140 terms is needed to achieve reliable approximation. A practical approximation can be obtained even with as little as 10-15 terms in the truncated series. This demonstrates the efficiency of the proposed technique both for monotone shapes and for shapes with decaying oscillatory shapes. The latter is of importance for the future application of the CON system used in the present work.

Acknowledgement. This work is supported by Grant LEQSF(1999-2002)-RD-A-49 from the Louisiana Board of Regents.

REFERENCES

- [1] K. L. Bekyarov and C. I. Christov. Fourier-Galerkin numerical technique for solitary waves of the fifth-order KdV equation. *Chaos, Solitons & Fractals*, 1:423-430, 1992.
- [2] J. P. Boyd. Spectral methods using rational basis functions on an infinite interval. *J. Comp. Phys.*, 69:112-142, 1987.
- [3] J. P. Boyd. *Chebyshev and Fourier Spectral Methods*. Springer, New York, 1989.
- [4] J. P. Boyd. The orthogonal rational functions of Higgins and Christov and algebraically mapped Chebishev polynomials. *J. Approx. Theory*, 61:98-105, 1990.
- [5] J. P. Boyd. Weakly nonlocal solitons for capillary-gravity waves: Fifth-Degree Korteweg-de Vries equation. *Physica, D* 48:129-146, 1991.
- [6] C. Canuto, M. Y. Hussaini, A. Quarteroni, and T. A. Zang. *Spectral Methods in fluid dynamics*. Springer, 1987.
- [7] M. Christou and C. I. Christov. Fourier-galerkin method for localized solutions of equations with cubic nonlinearity. *Journal of Computational Analysis and Applications*, 2000. To appear.
- [8] C. I. Christov. A complete orthonormal sequence of functions in $L^2(-\infty, \infty)$ space. *SIAM J. Appl. Math.*, 42:1337-1344, 1982.
- [9] C. I. Christov. A method for treating the stochastic bifurcation of plane poiseuille flow, nonlinear stochastic systems. *Ann. Univ. Sof., Fac. Math. Mech.*, 76(1b.2 - Mecanique):87-113, 1982.
- [10] C. I. Christov. Fourier-Galerkin algorithm for 2D localized solutions. *Annuaire de l'Univ. Sofia, Livre 2 - Mathématiques Appliquée et Informatique*, 89:169-179, 1995.
- [11] C. I. Christov and K. L. Bekyarov. A Fourier-series method for solving soliton problems. *SIAM J. Sci. Stat. Comp.*, 11:631-647, 1990.
- [12] C. I. Christov, G. A. Maugin, and M. G. Velarde. Well-posed Boussinesq Paradigm with purely spatial higher-order derivatives. *Phys. Rev. E*, 54:3621-3638, 1996.
- [13] T. Kawahara. Oscillatory solitary waves in dispersive media. *J. Phys. Soc. Japan*, 33:260-264, 1972.
- [14] N. Wiener. *Extrapolation, Interpolation and smoothing of stationary time series*. Technology Press MIT and John Wiley, New York, 1949.
- [15] Y. Yamamoto. Head-on collision of shallow-water solitary waves near the critical depth where dispersion due to gravity balances with that due to surface tension. *J. Phys. Soc. Japan*, 58:4410-4415, 1989.

DEPARTMENT OF MATHEMATICS, UNIVERSITY OF LOUISIANA AT LAFAYETTE, LAFAYETTE, LA 70504-1010, USA